Desalination and Water Treatment
www.deswater.com
doi: 10.1080/19443994.2013.765364

51 (2013) 5974–5986
September

Taylor & Francis
Taylor & Francis Group

Coalescing filtration of oily wastewaters: characterization and application of thermal treated, electrospun polystyrene filters

Mohammad Javad A. Shirazi[a,*], Saeed Bazgir[b], Mohammad Mahdi A. Shirazi[c], Seeram Ramakrishna[d]

[a]*Young Researchers and Elites Club, Science and Research Branch, Islamic Azad University, Tehran, Iran*
Tel./Fax: +98 (21) 44869752; email: mj.shirazi@srbiau.ac.ir
[b]*Nanopolymer Research Laboratory (NRL), Department of Polymer Engineering, Science and Research Branch, Islamic Azad University, Tehran, Iran*
[c]*Young Researchers and Elites Club, Omidieh Branch, Islamic Azad University, P.O. Box 164, Omidieh, Iran*
[d]*Center for Nanofibers & Nanotechnology (NUSCNN), National University of Singapore, Blk E3, #05-29, 2 Engineering Drive 3, Singapore 117576, Singapore*

Received 18 November 2012; Accepted 3 January 2013

ABSTRACT

In this study, a number of electrospun nanofibrous polystyrene (PS) filters were developed and applied for coalescing filtration of an oily wastewater stream at pilot scale. The effect of thermal treating on the morphology and performance of electrospun nanofibrous filters was studied. The initial effect of thermal treating started after 130°C and the maximum allowable thermal treating temperature observed was 150°C. The results obtained indicated that thermal treating led to the formation of uniform pore structure and pore size distribution, lower pore size, lower pore tortuosity, as well as higher coalescing filtration efficiency. Moreover, the surface roughness and surface energy decreased after thermal treating. To the best of our knowledge, this was the first attempt to use thermal treated electrospun nanofibrous PS filters at pilot-scale liquid–liquid coalescing filtration of oily wastewaters.

Keywords: Coalescing filtration; Electrospun nanofibrous filters; Thermal treating; Polystyrene; Characterization

1. Introduction

When two liquids are immiscible in one other, they can form either an emulsion or a colloidal suspension. In either of these mixtures, the dispersed liquid forms droplets in the continuous phase. In colloidal suspension, the droplets are less than 1 μm, in diameter, and the phases cannot readily be separated naturally. On another hand, emulsions divided into two major categories involve primary emulsion and secondary emulsion. Dispersed droplets in the first type typically have diameters more than 100 μm while in the secondary emulsions, droplet diameter typically decreased from 100 to 1 μm [1–3]. Both the colloidal suspensions and the secondary emulsions are serious challenges for different industries due to their stability and difficulty of separation through the conventional methods [4–7].

In the case of oily wastewaters (usually oil-in-water emulsions), fine divided oil droplets are, almost uniformly, dispersed in water as the continuous phase. The most conventional method commercially available for the treatment of oily emulsions involves chemical demulsification followed by air floatation

*Corresponding author.

[8,9]. This system needs to use expensive special chemicals and it produces sludge that has to be disposed of. Several physical methods are also used for the treatment of such kind of wastes in a more conventional way such as centrifugation, packed bed or electrolytic cells [10]. Liquid–liquid coalescing filtration is a versatile method which accelerates the merging of many droplets to form a lesser number of droplets, but with greater diameter [2,7,10]. This phenomenon can be explained by the well-known Stock's law which expresses that the falling or rising velocity of droplets as follows

$$\upsilon_d \propto \frac{R^2 g(\rho_d - \rho_f)}{9\mu} \quad (1)$$

where υ_s is the falling or rising velocity, R is droplets radius, ρ_d is the droplets density, and ρ_f is the fluid medium density. Settling/rising of the larger droplets downstream of the coalescing system then requires considerably less residence time [11,12]. Droplets coalescing involve three major steps: (a) droplets strike target and adhere, (b) several captured droplets coalesce on the medium, and (c) forming larger drops which trickle down/up and becoming separated. Therefore, coalescing medium is the most important part of a coalescing filtration system.

Electrospinning (ES) method has been applying to develop membranes [13–16] and filters [2,10,11,17–20] for various applications. Thavasi et al. [21], Pham et al. [22], Balamurugan et al. [23], and Nataraj et al. [24] published a number of reviews for various aspects of ES of polymers. Great worldwide attention to the ES method was observed because this technique is a simple and versatile method that creates fibers in the range of micron- to nano-size through an electrically charged jet of a polymer solution [25,26]. Various parameters such as operating parameters [27], solvent system [28,29], and type of applied needle [30] affect the morphology and the structure of nanofibrous mediums.

In this study, a number of electrospun nanofiber filters made of polystyrene (PS) were developed for coalescing filtration of secondary emulsion of oil in water at pilot scale. Thermal treating was used to prepare filters with more uniform pores and durable structure. Comprehensive morphology observations via scanning electron microscopy (SEM) and atomic force microscopy (AFM) analyses were carried out. The variation of surface energy was measured by use of contact angle (CA) analysis. The effect of thermal treating on the chemical stability of electrospun filters was studied by use of Fourier transform infrared spectroscopy (FTIR) analysis. The thermal behavior and crystal formation in electrospun fibers' structure, before and after thermal treating procedure were measured by differential scanning calorimetry (DSC). To the best of our knowledge, this was the first attempt to use thermal treated electrospun nanofibrous PS filters at pilot scale liquid–liquid coalescing filtration of oily wastewaters.

2. Materials and methods

2.1. Materials

PS granules (190,000Mw, Sigma–Aldrich, USA) were dissolved in *N*,*N*-Dimethylacetaminde (DMAc) (Merk, Germany) in order to prepare 20 wt.% polymer solution, as proper concentration for ES of PS [29]. Tetraethylammonium bromide salt (Merk, Germany) was used as an additive to prevent the beads formation [31,32]. Kerosene (Tehran Refinary Co., Iran) was used to synthesize oily wastewater.

2.2. ES and thermal treating procedure

An ES setup (Fig. 1) was used for fabrication of electrospun nanofibrous PS filters. About 18 kV electrical power was supplied by a Gamma high voltage power supply system (ES60P-5W, USA) between a stainless steel needle tip (18 gage) as nozzle and a collecting surface with 17 cm distance. The polymer solution was electrospun with the flow rate of 0.1 ml/min for 30 min in the preparation of each filter. All nanofibrous mats were kept in a fume hood for 48 h to dry at environmental conditions. ES system was worked at environmental temperature (25˚C) and pressure and 20–25% relative humidity.

A vacuum oven (Memmert, Germany) (in order to prevent surface oxidation and change in surface chemical composition), was used for 30 min thermal treating of nanofibrous filters under 90, 100, 120, 130, 140, 150, 160, and 170˚C temperatures, respectively.

2.3. Analysis

Based on the application, different specifications and properties of filters and membranes are required. In other words, surface properties have been described as direct influencing factors on the filter's and membrane's performance [33]. As occurred in other membrane-based separation processes, the successful application of coalescing filtration may be aided by a proper knowledge of the properties of the applied filter [34].

2.3.1. AFM and SEM characterization

There are several research studies using various analyzing methods, mainly SEM and AFM analyses, to describe surface topography [33–35]. Besides the

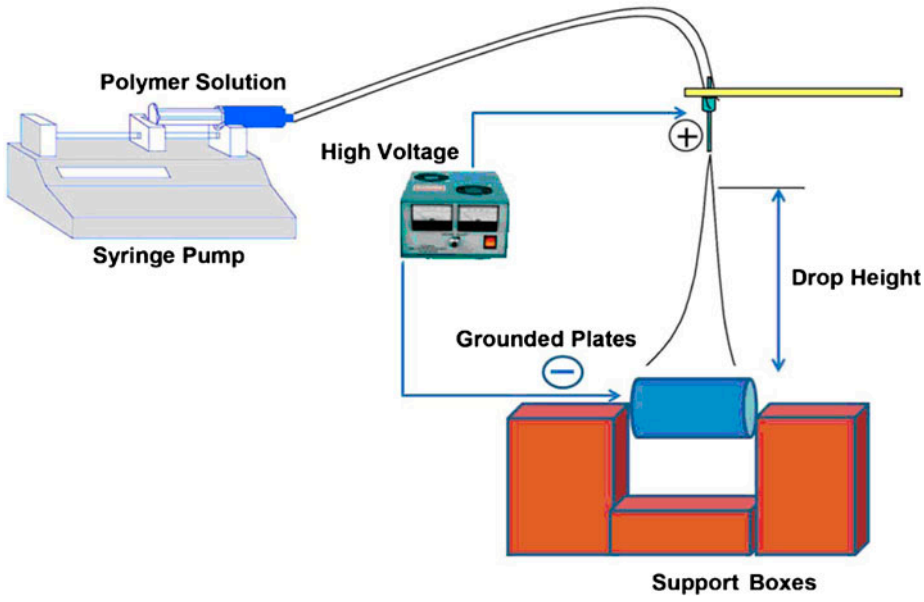

Fig. 1. A general scheme of the ES setup applied in this work.

well-known technique of SEM, AFM is a relatively new and emerging high resolution method to study the surface morphology of the separation filters and membranes [36]. Three-dimensional (3D) topographical images of the surface up to the atomic level by scanning a sharp tip can be achieved by AFM. The most important advantage of this method, other than the high resolution images, is that heavy metal coating (special sample preparation)—which is required in SEM and which may lead to some surface damage—is not necessary. HITACHI S-4160 SEM system with a voltage of 15.0 kV analyzing (Japan) and DUALSCOPE 95-200E AFM system with non-contact mode (DEM, Denmark) were used for morphology observation. SEM images were analyzed for fibers diameter, pore size, and pore size distribution, and porosity by use of Image Analyzer Software (Digimizer, Version 4.2.0.0). Roughness parameters were measured from AFM images.

2.3.2. Hydrophobicity characterization

Hydrophobicity of heterogeneous solid surfaces is usually measured by CA between the surface and a liquid droplet (mostly water). Analysis of the surface CA for the electrospun filters were performed by the use of a CA measuring system (KRUSS G-10, Germany).

2.3.3. Chemical stability

FTIR analysis (BRUKER EQUINOX-55 FTIR (Germany) (wavelengths ranging from 4,000 to 500 cm^{-1})) for electrospun filters were performed (via infrared absorption spectra) to study the effect of thermal treating on the chemical stability of nanofibers' surface, before and after thermal treating.

2.3.4. Thermal behavior characterization

Differential scanning calorimetric (DSC) is a thermoanalytical method in which the difference in the amount of heat required to increase the samples' temperature (electrospun nanofibrous filters in this work) as a function of the temperature, which can be used for analysis of the thermal behavior and the crystal formation in the nanofibrous structure. DSC analysis of electrospun filters, before and after thermal treating, were performed using TA-Instrument DSC-2010 system (USA) from 0℃ until thermal degradation of the samples at 175℃.

2.3.5. Coalescing filtration efficiency test

Coalescing filtration efficiency tests were performed using synthesized oily wastewater (prepared by dispersing kerosene (37 ml) (Tehran Refining Co.) in distilled water (30,000 ml)) by use of each electrospun PS filter. A pilot-scale filtration system, with 800 l/h maximum capacity, was used for experiments. Fig. 2 shows the coalescing filtration setup which contains: a centrifugal pump for feed stream, two stainless steel tanks for feed and the permeate, a precious flow-meter for feed-flow-rate adjustment, a precious

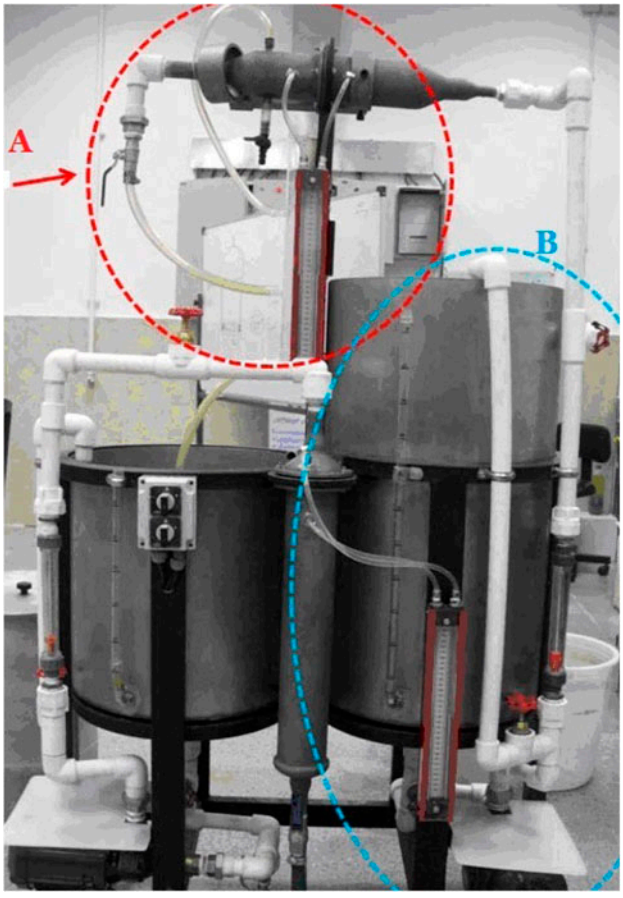

Fig. 2. Pilot scale coalescing filtration setup applied in this work (part A: horizontal filter housing and manometer, part B: baffled feed tank, mixer (located in the tank), flowmeter).

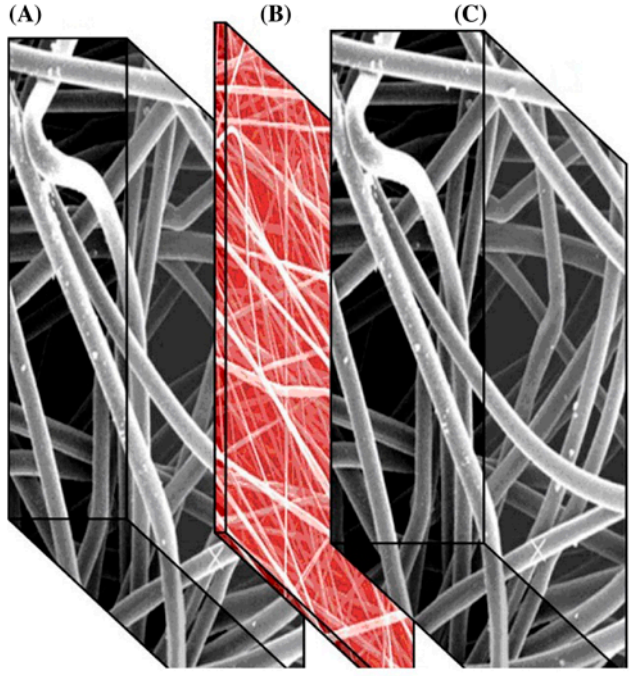

Fig. 3. The arrangement of composite nanofibrous filter, ((a) and (c): non-woven polyester layers, (b): electrospun nanofibrous PS layer).

manometer for pressure-drop measurement between two sides of the filter medium, an in-line decanter for separation evaluation after coalescing, and a dead-end filter housing made of stainless steel. The housing was divided into two parts and composite nanofibrous filter was fixed in the middle side. A perforated stainless steel structure was used as support for the filter medium. Fig. 3 shows the arrangement of the composite nanofibrous filter. Each experiment was run for 12 min with the constant flow rate of 1401/h. Particle size analyzing (CILAS-1064 particle size analyzer) test was performed, for the feed and the filtered samples, to evaluate oil droplets distribution.

3. Results and discussion

3.1. SEM analysis

Various parameters affect the morphology of the electrospun filters including type and molecular weight of polymer (PS in this work); solution parameters, ES conditions, and the ambient conditions such as temperature and humidity. ES through various mentioned conditions usually lead to three major morphologies including beaded structure, bead on string structure, and fiber structure (with ribbon or cylindrical shape). As it could be observed in Fig. 4((a) and (b)), randomly nanofibers—with the average diameter of 452 nm—were fabricated, while no beads were observed in the fibrous mat network. Fig. 5 shows the fibers' diameter and pore size distribution of electrospun filters. As it could be observed (Fig. 5(a)), about 40% of fibers were in the range of 400–500 nm, and about 27.5% of fibers were in the range of 300–400 nm. There were no fibers in the range of 0–200 nm and more than 800 nm. Moreover, the fabricated fibers had a smooth surface (Fig. 4(b)).

In order to study the effect of thermal treatment on the morphology of electrospun nanofibrous filters, 30 min thermal treating, and 90–170°C with 10°C elevation range, was carried out. During 90–130°C, no significant change was observed in the morphology of nanofibrous mats. For instance, Fig. 4(c) and (d) shows the SEM images of the filters after 90 and 120° C thermal treating, and no merging has happened among the fibers. However, analyzing the SEM images indicated that a minor change in the mean

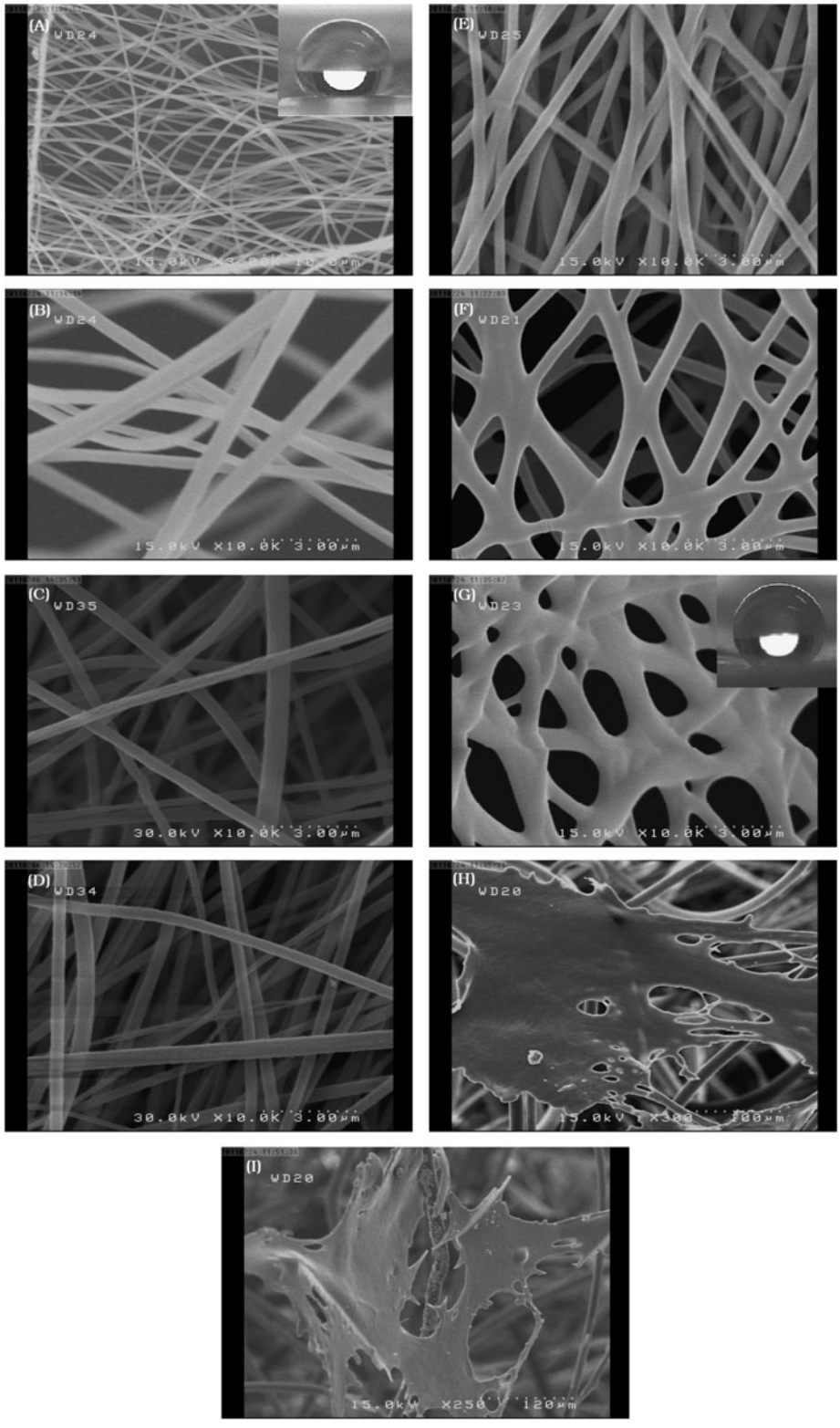

Fig. 4. SEM images showing the morphology of the electrospun nanobibrous filter, before thermal treating (a and b) (with two magnification); and after (c) 90˚C; (d) 120˚C; (e) 130˚C; (f) 140˚C; (g) 150˚C; (h) 160˚C; and (i) 170˚C thermal treating, respectively.

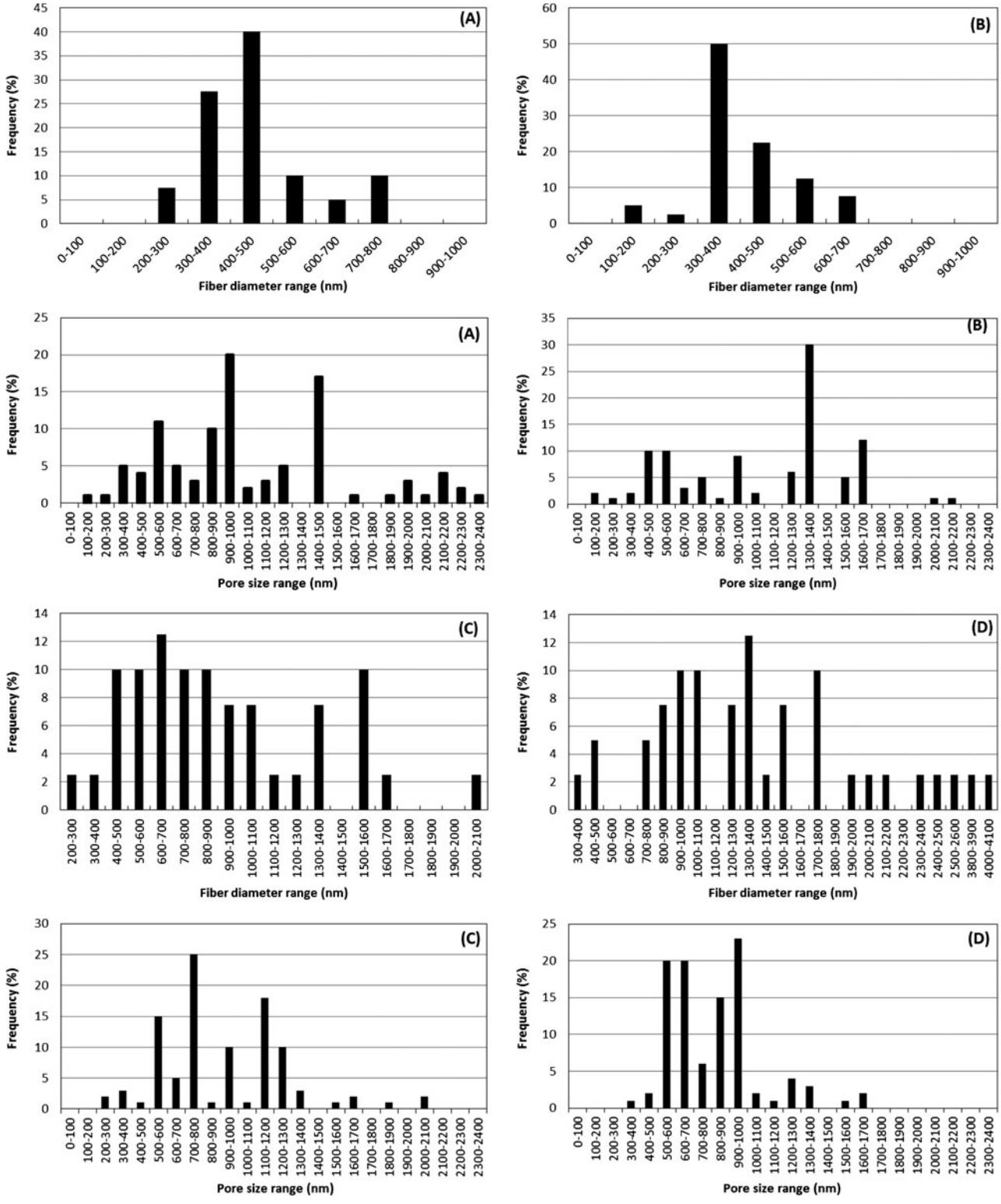

Fig. 5. Fibers diameter distribution and pore size distribution of the electrospun nanofibrous filters before (a) and after 130℃ (b), 140℃ (c), and 150℃ (d) thermal treating.

Table 1
Fibers' diameter range of electrospun filters before and after thermal treating

Fibers diameter (μm)	Before thermal treating	90°C	100°C	120°C	130°C	140°C	150°C	160°C⩽
Max	0.790	0.960	1.434	0.876	0.697	2.092	4.076	Degradation
Min	0.201	0.227	0.176	0.103	0.117	0.234	0.396	Degradation
Mean	0.412	0.491	0.644	0.460	0.412	0.943	1.456	Degradation

fibers' diameter was achieved after thermal treating. Table 1 presents the measured values for mean fibers' diameter before and after thermal treating operation. It is worth noting that fibers' mean diameter was increased by thermal treating up to 100°C, while it was decreased after 120°C and was increased again up to 150°C. Experimental results indicated that the maximum allowable temperature for thermal treating of electrospun nanofibrous PS filters was 150°C. Higher operating temperatures led to thermal degradation of the electrospun structure (Fig. 4(h) and (i)).

The pores' structure is one of the major characteristics of synthesized filters and membranes which should be considered. As it could be observed in Fig. 4, thermal treating led to a more uniform pore structure and the best configurations were achieved after 130–150°C thermal treating (Fig. 4(g)). In other words, the pore tortuosity (which is defined as the degree of deviation of the pore structure from a straight cylindrical shape) decreased after thermal treating operation in comparison with non-thermal treated electrospun filter. Moreover, the porosity of 150°C thermal treated filter decreased to 61.6%. It could be explained by this fact that after thermal treating, the nanofibers start to merge together. As it could be observed in Fig. 4, increasing the thermal treating temperature led to increase in the fibers' merging up to 150°C. The maximum, the minimum, and the mean pore size after 150°C thermal treating were 3.44, 0.151, and 1.018 μm; while these values for the non-thermal treated and the 130°C thermal treated filters were 2.359, 0.262, and 1.008 μm; and 1.650, 0.207, and 0.648 μm; respectively.

Fig. 5 shows the fiber diameter range and the pore size distribution of electrospun filters, before and after thermal treating. As it could be observed, about 40% of fibers were in the range of 400–500 nm before thermal treating, while after 130°C, thermal treating about 50% of the fibers were in the range of 300–400 nm. However, after 140 and 150°C, thermal treating a number of fibers with wide ranges of diameter distribution were observed (Fig. 5(c) and (d)). This was due to fibers' merging with increase in the thermal treating temperature.

Before thermal treating, about 20 and 17% of pores were in the range of 900–1,000 nm and 1,400–1,500 nm, respectively. After 130°C thermal treating, about 30% of the pores were in the range of 1,300–1,400 nm; while after 140°C thermal treating, 20 and 16% of the pores were in the range of 700–800 nm and 1,100–1,200 nm, respectively. As it could be observed in Fig. 5(d), after 150°C thermal treating the more uniform pore size distribution was achieved, and about 23% of the pores were in the range of 900–1,000 nm. It is worth quoting that 20% of pores were in the ranges of 500–600 nm and 600–700 nm.

Generally speaking, it could be concluded that the thermal treating operation had considerable effect on the electrospun filters' structure, and directly affected the fibers' diameter, porosity, tortuosity, 3D-interconnected structure, and pore size and pore size distribution. In other words, increasing the thermal treating temperature up to 150°C led to an increase in the fibers' diameter while decreasing the pore size. Moreover, uniform fibers' diameter and pore sizes' distribution as well as lower pores' tortuosity were achieved after thermal treating.

3.2. AFM analysis

Researches in the past years have demonstrated the power of AFM for characterization of polymeric membranes [33,34]. Therefore, non-contact mode of AFM was used for characterization of surface roughness, and phase study of elecrospun PS filters, before and after 150°C thermal treating operation. Fig. 6 shows the two dimensional (2D) AFM and phase images of electrospun filters.

In the first step, the filters were characterized for their surface roughness. Surface roughness is an important property which directly affects the surface hydrophobicity and the fouling potential of membranes and filters. Various roughness parameters such as the mean roughness (R_a), the root mean square of Z data (R_q), and the mean difference in the height between the five highest peaks and the five lowest valleys (R_z) measured. These parameters were obtained from the AFM images of different locations

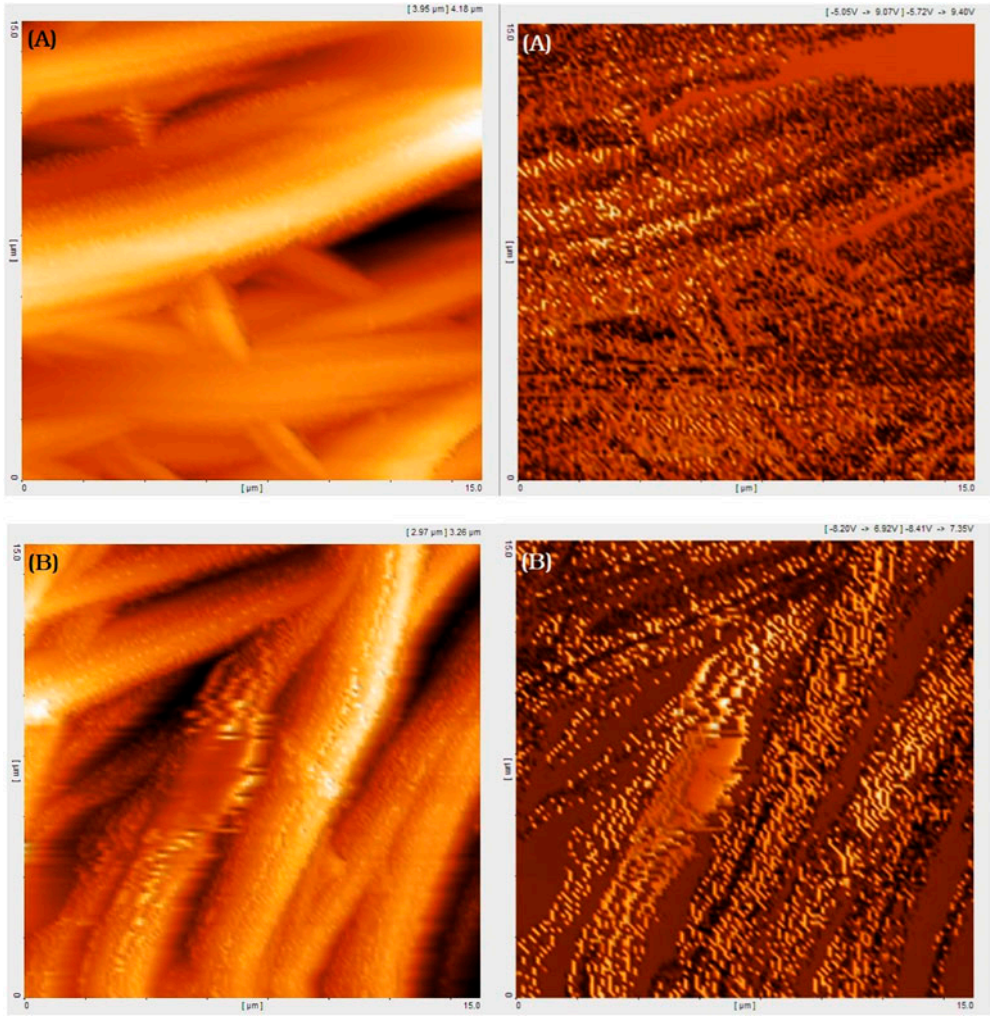

Fig. 6. 2D AFM and phase images of electrospun PS filters (a) before and (b) after 150˚C thermal treating, (AFM images in the left side and phase images in the right side).

taken from the 2×2 cm filter samples, and then the average values were reported. R_a represents the mean value of the surface relative to the center plane for which the volumes enclosed by the images above and below this plane are equal. R_q is the standard deviation of the Z values within the specific area. Table 2 shows these roughness parameters. As it could be observed in Fig. 6, the filters' surface was not smooth and some nodule aggregates were observed. The nodules are seen as bright high peaks while pores are seen as darker depressions. As in ES, a charged jet of polymer solution erupts from the needle tip to the collecting surface and randomly fibers make a non-woven filter; therefore, pores are not necessarily circular. It is worth noting that the thermal treating changed the pores' and structure, and decreased the surface roughness. It can be explains by the fact that during ES, the solvent evaporates and a solid polymeric fiber is formed. This evaporation, especially from the sub-layers to the fiber's surface, increases the nanometric nodules on the fibers' body, which leads to an increase in the roughness. When thermal treating operation was carried out, nanofibers merged

Table 2
The roughness parameters of electrospun PS filters, before and after 150˚C thermal treating

Parameters	R_a (nm)	R_z (μm)	R_q (nm)
Before thermal treating	290	1.71	354
After 150˚C thermal treating	230	1.35	246

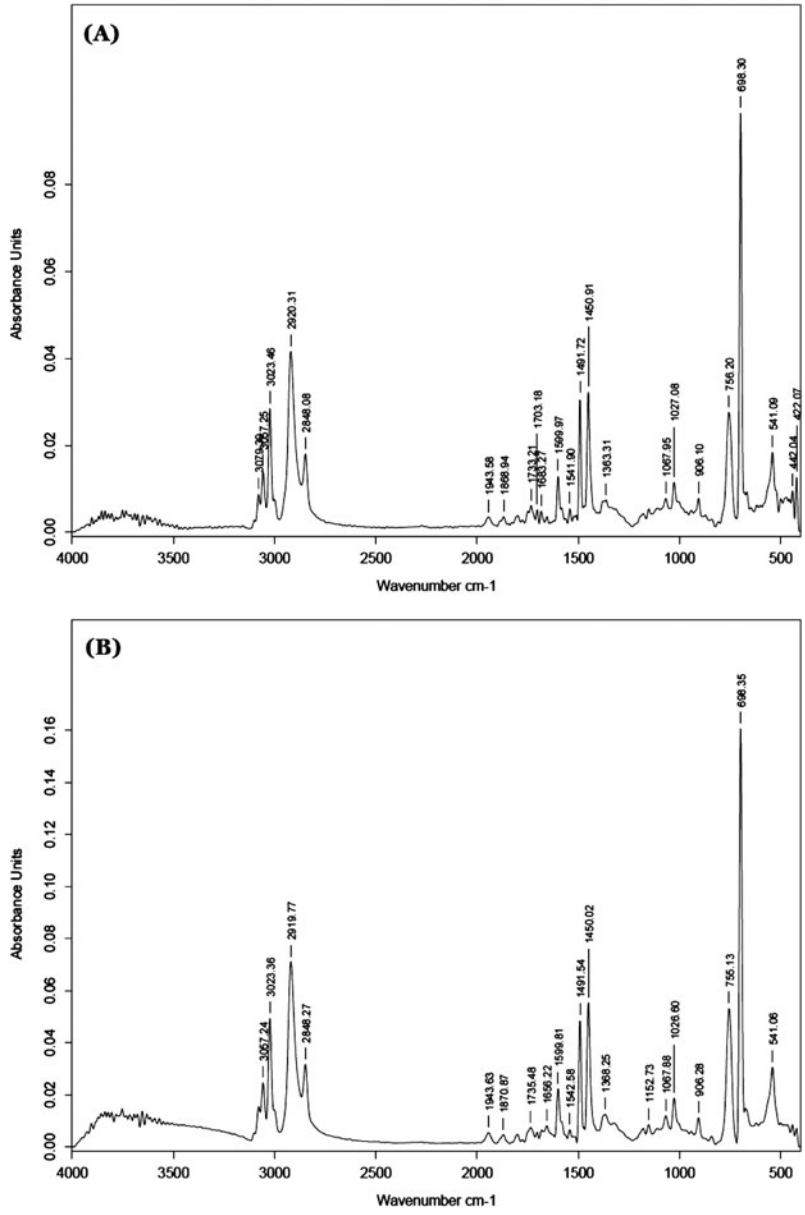

Fig. 7. The FTIR analysis of electrospun PS filters (a) before and (b) after 150˚C thermal treating.

together and microfibers were formed without nodules on the surface. This led to a smoother surface. Moreover, as it is explained in Section 3.1, pores with more uniform structure and lesser tortuosity were achieved after thermal treating.

One of the abilities of AFM is introducing the phase image of scanned samples. As the dop solution for ES is at least a binary solution (mixture of polymer and solvent), phase images observation can be investigated as an effective method for phase distribution observation. It could be observed in Fig. 6 that after thermal treating, the distribution of the condensed phase (PS) increased in comparison with the electrospun filter before thermal treating. It can be explained by thes fact that thermal treating led to evaporate the trace of trapped solvent in the fibers' body during their merging.

3.3. FTIR analysis

Beyond structural analysis of the electrospun filters via SEM and AFM, the chemical compositions were

investigated before and after 150˚C thermal treating. Fig. 7 shows the infrared absorption spectra, with wavelengths ranging from 4,000 to 500 cm^{-1}. As it could be observed, thermal treating did not change the chemical structure of electrospun filters due to vacuum condition of applied oven during thermal treating operation. However, one of the major effects of thermal treating could be the increase in the mechanical stability of electrospun filters through changing the three-dimensional detached interconnected structure to a more durable two dimensional merged fibers structure.

3.4. Hydrophobicity analysis

Hydrophobicity of membranes is usually measured by CA between the membrane's surface and water droplet. Various parameters affect the surface hydrophobicity, which is described elsewhere [37]. In order to study the effect of ES and thermal treating on the hydrophobicity of electrospun filters, the intrinsic hydrophobicity of PS was measured through preparation of thin film of PS via solution-casting of PS/DMAc solution on a glass surface. As the CA could be observed in Fig. 8, the fabricated PS film with 88.6 ± 0.5˚ CA was relatively hydrophobic. Obviously, ES increased the filter's CA up to 135.5 ± 0.5˚. This result supports the hypothesis that ES increases the hydrophobicity of polymers. Moreover, after 150˚C thermal treating, the CA of electrospun mat increased up to 156 ± 0.5˚. It is worth quoting that based on Cassie–Baxter theory, for a heterogeneous surface, increase in the surface roughness leads to an increase in the hydrophobicity. It should be noted that the thermal treating operation decreased the roughness on the fibers' surface, while the overall surface's roughness of the electrospun filters increased after thermal treating.

3.5. Coalescing filtration efficiency test

A coalescing filtration efficiency test using synthesized oily wastewater (secondary emulsion of kerosene in distilled water) was performed, on which the dispersed phase (oil droplets) was seen as small droplets with average diameter of 31.54 μm. This test aimed to evaluate the effect of thermal treating on the coalescing filtration efficiency of the electrospun PS filters. The oily wastewater separation in this work involved three major parts, adsorbing on the filter's surface, screening, and coalescing of fine droplets and releasing of larger ones as floating layer. As the aim of this work was studying the effect of thermal treating on the coalescing filtration performance of electrospun PS filters, an in-line decanter was used to evaluate the coalescing separation efficiency. Particle size test was carried out for analyzing the feed and the filtrated samples. Fig. 9 shows the original scanned graphs of laser particle size analyses for the feed and the filtrated samples obtained after using a single non-woven layer, a non-thermal treated, and thermal treated filters, respectively. As it could be observed, the average diameter of oil droplets after coalescing separation using a single non-woven layer decreased down to 5.19 μm. Same value was obtained after using the nanofibrous coated non-woven mat; although, the separated oil was 7 and 8.5 ml (in volume), respectively. Using 130˚C thermal treated electrospun filter, the permeate sample contained droplets with average diameter of 5.69 μm and 9 ml oil separated. As it could be observed in Fig. 10, the increase in the thermal treating temperature led to an increase in the volume of separated oil in the in-line decanter up to 13 ml. It is worth noting that these results for separations were obtained during about 14 min operating time, while natural separation for the same feed sample—which was experimented in a sealed graduated cylinder— took 96 h. It means that using thermal treated electrospun PS filters significantly increased

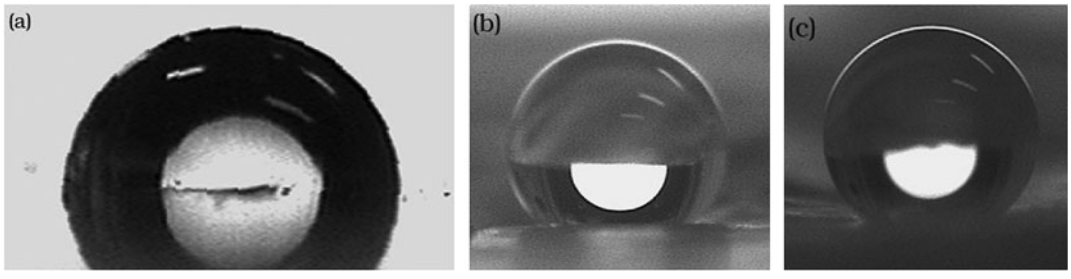

Fig. 8. The CA of (a) PS film (fabricated via solution-casting of PS/DMAc solution and environmental conditions (88.6 ± 0.5˚)); (b) electrospun nanofibrous membrane before thermal treating (135 ± 0.5˚); and (c) after thermal treating (156 ± 0.5˚).

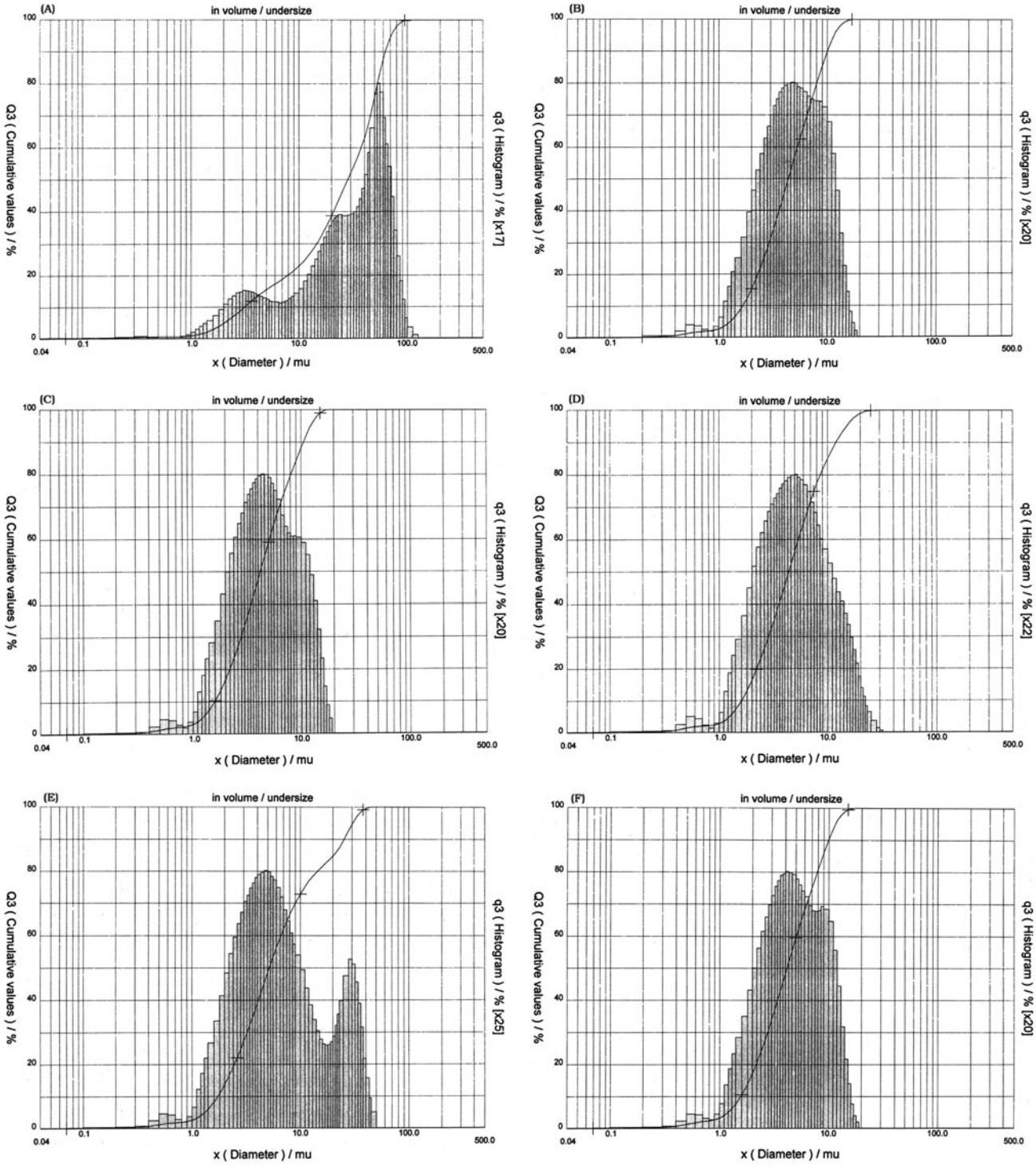

Fig. 9. The results of particle size analyzing of the applied feed (a), and permeate by use of non-woven (b), non-thermal treated electrospun (c), 130˚C thermal treated (d), 140˚C thermal treated (e), and 150˚C thermal treated (f) filters, respectively.

the separation efficiency and decreased the required operating time, which directly influenced the operating costs and the overall process efficiency.

4. Conclusions

Coalescing filtration is one of the major unit operations in chemical industries, especially in the case of

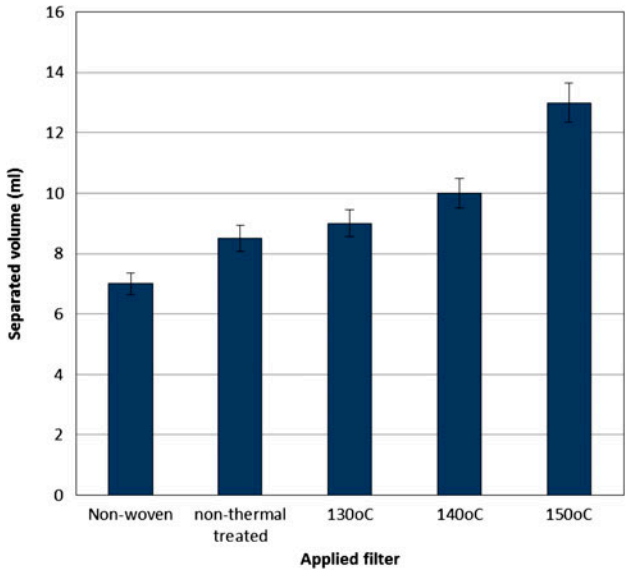

Fig. 10. The separated volume in the permeate phase vs. the type of applied filter.

oily wastewater treatment. As the coalescing medium has a critical role, development of new filters with better performance is a critical subject. Following points are concluded based on the results obtained in this work:

- ES is a versatile and could be considered as an emerging method for fabrication of highly porous coalescing filters with three-dimensional interconnected pore structure.
- Characterization of electrospun coalescing filters could provide in-depth knowledge of these filters' performance.
- AFM method, besides SEM, FTIR, etc., could effectively be used for characterization and morphological study of the electrospun coalescing filters.
- Thermal treating led to formation of more uniform pores, lower tortuosity, lower porosity, and lower surface roughness of fibers, lower pore size, and better coalescing filtration performance.
- Thermal treating of electrospun filters up to 150°C led to higher coalescing separation efficiency.
- The maximum allowable temperature for thermal treating of electrospun PS filters observed was 150°C, and further increase in temperature led to thermal degradation.
- Thermal treated electrospun PS filters were successfully applied for the coalescing filtration of oily wastewater.

Acknowledgments

We acknowledge the financial support provided by Young Researches and Elites Club (Science and Research Branch of Islamic Azad University, Tehran) for this work.

References

[1] R. Pal, Techniques for measuring the composition (oil in water content) of emulsions, a state of the art review, Colloid Surf. A: Physicochem. Eng. Aspects 84 (1994) 141–193.
[2] C. Shin, G.C. Chase, D.H. Reneker, The effect of nanofibers on liquid–liquid coalescence filter performance, AIChE J. 51 (2005) 3109–3113.
[3] T.H. Wines, R.L. Brown, Difficult liquid–liquid separation: High-performance, polymer-fiber coalescers break up hard-to-handle emulsions and dispersions, Chem. Eng. (1997).
[4] F.R. Ahmadun, A. Pendashteh, L.C. Abdulah, D.R.A. Biak, S. S. Madaeni, Z.Z. Abidin, Review of technologies for oil and gas produced water treatment, J. Hazard. Mater. 170 (2009) 530–551.
[5] M. Takht Ravanchi, T. Kaghazchi, A. Kargari, Application of membrane separation processes in petrochemical industry: A review, Desalination 235 (2009) 199–244.
[6] T. Mohammadi, A. Ezzati, E. Gorouhi, Separation of water in oil emulsions using microfiltration, Desalination 185 (2005) 371–382.
[7] R.S. Barhate, S. Sundarrajan, D. Pliszka, S. Ramakrishna, Fine chemical processing: The potential of nanofibers in filtration, Filtr. Sep. 45 (2008) 32–35.
[8] V.B. Menon, D.T. Wasan, Demulsification, In: P. Becher (Ed.), Encyclopedia of Emulsion Technology, Marcel Dekker, New York, NY, pp. 1–75, 1985.
[9] A.D. Nikolov, M. Randie, C.S. Shetty, D.T. Wasan, Chemical demulsification of oil-in-water emulsion using air floatation: The importance of film thickness stability, Chem. Eng. Commun. 152–153 (1996) 337–350.
[10] A. Hong, A.G. Fane, R. Burford, Factors affecting membrane coalescence of stable oil-in-water emulsions, J. Membr. Sci. 222 (2003) 19–39.
[11] A.L. Yarin, G.G. Chase, W. Liu, S.V. Doiphode, D.H. Reneker, Liquid drop growth on a fiber, AIChE J. 52 (2006) 217–227.
[12] J. Eggers, J.R. Lister, H.A. Stone, Coalescence of liquid drops, J. Fluid Mech. 401 (1999) 293–310.
[13] S. Kaur, D. Rana, T. Matsuura, S. Sundarrajan, S. Ramakrishna, Preparation and characterization of surface modified electrospun membranes for higher filtration flux, J. Membr. Sci. 390–391 (2012) 235–242.
[14] A. Patanaik, V. Jacobs, R.D. Anandjiwala, Performance evaluation of electrospun nanofibrous membrane, J. Membr. Sci. 352 (2010) 136–142.
[15] S. Kaur, D. Rana, T. Matsuura, S. Sundarrajan, S. Ramakrishna, Influence of electrospun fiber size on the separation efficiency of thin film nanofiltration composite membrane, J. Membr. Sci. 392–393 (2012) 101–111.
[16] S.S. Homaeigohar, K. Buhr, K. Ebert, Polyethersulfone electrospun nanofibrous composite membrane for liquid filtration, J. Membr. Sci. 365 (2010) 68–77.
[17] C. Shin, G.G. Chase, D.H. Reneker, Recycled expanded polystyrene nanofibers applied in filter media, Colloids Surf. A: Physicochem. Eng. Aspects 262 (2005) 211–215.
[18] C. Shin, Filtration application from recycled expanded polystyrene, J. Colloid Interface Sci. 302 (2006) 267–271.
[19] H. An, C. Shin, G.G. Chase, Ion exchanger using electrospun polystyrene anofibers, J. Membr. Sci. 283 (2006) 84–87.
[20] C. Shin, G.G. Chase, Water-in-oil coalescing in micro-nanofiber composite filters, AIChE J. 50 (2004) 343–350.

[21] V. Thavasi, G. Singh, S. Ramakrishna, Electrospun naofibers in energy and environmental applications, Energy Environ. Sci. 1 (2008) 205–221.
[22] Q.P. Pham, U. Sharma, A.G. Mikos, Electrospinning of polymeric nanofibers for tissue engineering applications: A review, Tissue Eng. 12 (2006) 1197–11211.
[23] R. Balamurugan, S. Sundarrajan, S. Ramakrishna, Recent trends in nanofibers membranes and their suitability for air and water filtrations, Membranes 1 (2011) 232–248.
[24] S.K. Nataraj, K.S. Yang, T.M. Aminabhavi, Polyacrylonitrile-based nanofibers- a state-of-the-art review, Prog. Polym. Sci. 37 (2012) 487–513.
[25] G.C. Rultedge, S.V. Fridrikh, Formation of fibers by electrospinning, Adv. Drug Delivery Rev. 59 (2007) 1384–1391.
[26] J. Doshi, D.H. Reneker, Electrospinning process and applications of electrospun fibers, J. Electrostat. 35 (1995) 151–160.
[27] R. Jalili, S.A. Hosseini, M. Morshed, The effects of operating parameters on the morphology of electrospun polyacrilonitrile nanofibers, Iran. Polym. J. 14 (2005) 1074–1081.
[28] S. Tungprapa, T. Puangparn, M. Weerasombut, I. Jangchud, P. Fakum, S. Semongkhol, Ch. Meechaisue, P. Supaphol, Electrospun cellulose acetate fibers: Effect of solvent system on morphology and fiber diameter, Cellulose 14 (2007) 563–575.
[29] T. Jarusuwannapoom, W. Hongrojjanawiwat, S. Jitjaicham, L. Wannatong, M. Nithitanakul, C. Pattamaprom, P. Koombhongse, R. Rangkupan, P. Supaphol, Effects of solvents on electrospinnability of polystyrene solutions and morphological appearance of resulting electrospun polystyrene fibers, Eur. Polym. J. 41 (2005) 409–421.
[30] G. Gururajan, S.P. Sullivan, T.P. Beebe, D.B. Chase, J.F. Rabolt, Continuous electrospinning of polymer nanofibers of nylon-6 using an atomic force microscope tip, Nanoscale 3 (2011) 3300–3308.
[31] K.H. Lee, H.Y. Kim, H.J. Bang, Y.H. Juang, S.G. Lee, The change of bead morphology ormed on electrospun polystyrene fibers, Polymer 44 (2003) 4029–4034.
[32] G. Eda, S. Shivkumar, Bead structure variations during electrospinning of polystyrene, J. Mater. Sci. 41 (2006) 5704–5708.
[33] E.F. Barbosa, L.P. Silva, Nanoscale characterization of synthetic polymeric porous membranes: Scrutinizing their stiffness, roughness, and chemical composition, J. Membr. Sci. 407–408 (2012) 128–135.
[34] M.M.A. Shirazi, A. Kargari, M.J.A. Shirazi, Direct contact membrane distillation for seawater desalination, Desalin. Water Treat. 49 (2012) 368–375.
[35] S. Kaur, R. Barhate, S. Sundarrajan, T. Matsuura, S. Ramakrishna, Hot pressing of electrospun membrane composite and its influence on separation performance on thin film composite nanofiltration membrane, Desalination 279 (2011) 201–209.
[36] M.M.A. Shirazi, D. Bastani, A. Kargari, M. Tabatabaei, Characterization of polymeric membranes for membrane distillation using atomic force microscopy, Desalin. Water Treat. doi: 10.1080/19443994.2013.765365
[37] Ch.M. Chan, Polymer Surface Modification and Characterization, Hanser, New York, NY, 1994.